Inorg. Chem. **2007**, *46*, 11173–11182

fac-$[Re(CO)_3L]^+$ Complexes with N–CH_2–CH_2–X–CH_2–CH_2–N Tridentate Ligands. Synthetic, X-ray Crystallographic, and NMR Spectroscopic Investigations

Anna Maria Christoforou, Patricia A. Marzilli, Frank R. Fronczek, and Luigi G. Marzilli*

Department of Chemistry, Louisiana State University, Baton Rouge, Louisiana 70803

Received August 7, 2007

Polyamine ligands (**L**) have excellent binding characteristics for the formation of *fac*-$^{99m}Tc(CO)_3$-based radiopharmaceuticals. Normally, these **L** are elaborated so as to leave pendant groups designed to impart useful biodistribution characteristics to the *fac*-[$^{99m}Tc(CO)_3$**L**] imaging agent. Our goal is to lay a foundation for understanding the features of the bound elaborated ligands by using the *fac*-[$Re(CO)_3$**L**]-analogue approach with the minimal prototypical ligands, diethylenetriamine (dien) or simple dien-related derivatives. Treatment of the *fac*-$[Re(CO)_3(H_2O)_3]^+$ cation with such triamine (NNN) ligands afforded *fac*-$[Re(CO)_3L]^+$ complexes. Ligand variations included having a central amine thioether donor, thus allowing X-ray crystallographic and NMR spectroscopic comparisons of *fac*-$[Re(CO)_3L]^+$ complexes with NNN and NSN ligands. *fac*-$[Re(CO)_3L]^+$ complexes with two terminal *exo*-NH groups exhibit unusually far upfield *exo*-NH NMR signals in DMSO-d_6. Upon the addition of Cl^-, these *exo*-NH signals move downfield, while the signals of any *endo*-NH or central NH groups move very little. This behavior is attributed to the formation of 1:1 ion pairs having selective Cl^- hydrogen bonding to both *exo*-NH groups. Base addition to a DMSO-d_6 solution of *meso-exo*-$[Re(CO)_3(N,N',N''\text{-}Me_3dien)]PF_6$ led to isomerization of only one NHMe group, producing the chiral isomer. The meso isomer did not form. The $[Re(CO)_3(N,N,N',N'',N''$-pentamethyldiethylenetriamine)]triflate·$[Re(CO)_3(\mu_3\text{-}OH)]_4$·$3.35H_2O$ crystal, the first structure with a *fac*-$[Re(CO)_3L]$ complex cocrystallized with this well-known cluster, provided parameters for a bulky NNN ligand and also reveals CO–CO interlocking intermolecular interactions that could stabilize the crystal.

Introduction

Radiopharmaceuticals based on the *fac*-$[^{99m}Tc(CO)_3]^+$ core are gaining extensive use because the *fac*-$[^{99m}Tc(CO)_3(H_2O)_3]^+$ precursor can be conveniently generated.[1−4] Agents with a tridentately coordinated ligand (**L**) of the type *fac*-[$^{99m}Tc(CO)_3$**L**] are more robust and have better pharmacokinetic profiles than agents bearing mono- or bidentate ligands.[5] A recent straightforward preparation of aqueous solutions of the nonradioactive *fac*-$[Re(CO)_3(H_2O)_3]^+$ precursor[6] has made the synthesis of *fac*-[$Re(CO)_3$**L**] analogues convenient and allows simulation of the aqueous ^{99m}Tc synthetic chemistry.[6,7] (Note: All specific complexes mentioned in this work have a facial geometry; therefore, the *fac*- designation is used henceforth only for referring to a general class of compounds.) The most commonly employed **L**s contain N, O, and S as donor atoms from amine,[8−10] pyridyl,[11] carboxyl,[8] or thioether[6,7] groups. Extensively characterized *fac*-[$Re(CO)_3$**L**] complexes of a series of symmetric and nonsymmetric NNN or NSN ligands contain-

* To whom correspondence should be addressed. E-mail: lmarzil@lsu.edu.

(1) Alberto, R.; Schibli, R.; Egli, A.; Schubiger, P. A.; Abram, U.; Kaden, T. A. *J. Am. Chem. Soc.* **1998**, *120*, 7987−7988.
(2) Alberto, R.; Schibli, R.; Schubiger, A. P.; Abram, U.; Pietzsch, H. J.; Johannsen, B. *J. Am. Chem. Soc.* **1999**, *121*, 6076−6077.
(3) Alberto, R.; Schibli, R.; Waibel, R.; Abram, U.; Schubiger, A. P. *Coord. Chem. Rev.* **1999**, *192*, 901−919.
(4) Schibli, R.; Alberto, R.; Abram, U.; Abram, S.; Egli, A.; Schubiger, P. A.; Kaden, T. A. *Inorg. Chem.* **1998**, *37*, 3509−3516.
(5) Schibli, R.; La Bella, R.; Alberto, R.; Garcia-Garayoa, E.; Ortner, K.; Abram, U.; Schubiger, P. A. *Bioconjugate Chem.* **2000**, *11*, 345−351.
(6) He, H.; Lipowska, M.; Xu, X.; Taylor, A. T.; Carlone, M.; Marzilli, L. G. *Inorg. Chem.* **2005**, *44*, 5437−5446.
(7) He, H.; Lipowska, M.; Xu, X.; Taylor, A. T.; Marzilli, L. G. *Inorg. Chem.* **2007**, *46*, 3385−3394.
(8) Lipowska, M.; Cini, R.; Tamasi, G.; Xu, X. L.; Taylor, A. T.; Marzilli, L. G. *Inorg. Chem.* **2004**, *43*, 7774−7783.
(9) Mundwiler, S.; Candreia, L.; Hafliger, P.; Ortner, K.; Alberto, R. *Bioconjugate Chem.* **2004**, *15*, 195−202.
(10) Christoforou, A. M.; Fronczek, F. R.; Marzilli, P. A.; Marzilli, L. G. *Inorg. Chem.* **2007**, *46*, 6942−6949.
(11) Lazarova, N.; Babich, J. W.; Valliant, J.; Schaffer, P.; James, S.; Zubieta, J. *Inorg. Chem.* **2005**, *44*, 6763−6770.

10.1021/ic701576u CCC: $37.00 © 2007 American Chemical Society
Published on Web 11/29/2007

Chart 1

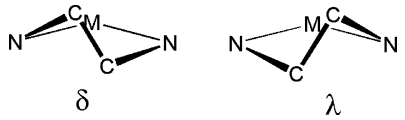

ing combinations of amine, pyrazolyl, and thioether donors are known.[12−14] During the development of radiopharmaceutical renal agents, polyamino-polycarboxylic acid ligands have been investigated.[8,15,16] At high pH, amine group coordination is preferred, allowing for dangling carboxyl groups, which are important in high renal clearance. Other studies involving nitrogen, sulfur, and oxygen donors have proposed that nitrogen donor ligands are better than sulfur donor ligands for *fac*-[Re(CO)$_3$**L**] complex formation.[11,17]

The location in space of the chelate ring atoms is a key factor in designing *fac*-[^{99m}Tc(CO)$_3$**L**] agents because these atoms act as a fulcrum for the pendant groups. In turn, the position of the pendant group has a significant effect on the overall shape of the agent[18] and hence on its biological activity. For diethylenetriamine-type ligands bound to a metal center in a tridentate fashion, the pucker of the two five-membered chelate rings can have either δ or λ chirality (Chart 1), leading to four possible combinations of chelate ring chirality, $\delta\lambda$, $\lambda\delta$, $\lambda\lambda$, and $\delta\delta$. X-ray structures from the Cambridge Structural Database of [M(dien)$_2$]$^{n+}$ (M = Ni, Co, Zn, Cu, Cr, Rh, Ir; dien = diethylenetriamine)[19] and of [M(dien)**L**$_n$][20] complexes and M(dien) fragments[21] were analyzed by principal component analysis (pca) studies, and the $\delta\lambda$ and $\lambda\delta$ conformation combinations were found more frequently than the $\delta\delta$ and $\lambda\lambda$ combinations. These results contradicted the Schmidtke and Garthoff[22] suggestion that a facially coordinated dien ligand favors a $\delta\delta$ or $\lambda\lambda$ combination because of steric effects of the hydrogen atoms on the ethylene chains.

In a previous study[10] we explored the chirality of the ligand pucker in a series of *fac*-[Re(CO)$_3$**L**] complexes with tridentate monoanionic ligands containing the diethylenetriamine moiety and an aromatic group connected through a sulfonamide group, such as *N*-[2-(2-aminoethylamino)ethyl]-2,4,6-trimethylbenzenesulfonamide (tmbSO$_2$-dienH) (Chart 2). (The H in the ligand names indicates the number of dissociable protons in the ligand and the complex.) We have also examined related complexes with elaborated dien ligands linked with CO in place of SO$_2$.[18] Our results showed that facially coordinated sulfonamido ligands have different chirality in each chelate ring more frequently than they have the same chirality, in agreement with the pca reports.[20,21] In contrast, the two chelate rings in the Re analogue of [^{99m}Tc(CO)$_3$(LANH)] agents (LANH$_2$ = lanthionine, a natural dicysteine-derived dipeptide linked through a common sulfur and exhibiting tridentate NSN binding) were found to have the same chirality.[7] The ^{99m}Tc-tagged lanthionine agents were the first small *fac*-[^{99m}Tc(CO)$_3$**L**] agents reported to have been evaluated in humans;[23] thus, additional studies directed at gaining a more comprehensive assessment of conformation are warranted.

Normally, the two protons of a primary amino group bound to a metal are magnetically inequivalent and are expected to have two separate ^{1}H NMR signals with similar shifts. The similarity in shifts is understandable because the inductive effects of the surrounding atoms on the amine nitrogen should be transmitted nearly equally to the protons. However, in several past studies we found unusually upfield- and (in fewer cases) downfield-shifted NH signals for *fac*-[Re(CO)$_3$**L**] complexes with terminal amino groups, (e.g., *fac*-[Re(CO)$_3$**L**] complexes of *S*-methyl-L-cysteine,[6] methionine,[6] *chiral*-LANH$_2$,[7] and sulfonamide ligands such as tmbSO$_2$-dienH),[10] whereas in some other cases (e.g., *fac*-[Re(CO)$_3$**L**] complexes of *meso*-LANH$_2$ and ethylenediamine-*N*-acetic acid, ENACH) the NH signals had similar shifts. The tridentate ligand in [Re(CO)$_3$(ENDAC)]$^-$ (ENDACH$_2$ = ethylenediamine-*N*,*N*′-diacetic acid, Chart 2) binds through a terminal amine group (NHCH$_2$CO$_2^-$) and a secondary NH group anchoring two chelate rings. Two isomers were crystallized, one with an *endo*-NH proton (pointing toward the carbonyl groups) and the other with an *exo*-NH proton (pointing away from the carbonyl groups).[8] In this study, we have examined *fac*-[Re(CO)$_3$**L**] complexes with less elaborate prototypical ligands, ones lacking large pendant substituents, in order to establish baseline behavior and thereby define parameters useful for assessing the effects of the pendant groups. These unusual shifts have led us to investigate the interaction of the complex with solvent as well as with the chloride anion. Such an investigation can be viewed as creating a very preliminary set of empirical observations relevant to the very difficult problem of predicting biodistribution, which is influenced by interactions of the agent with the solvent and the anions present in the media.

Experimental Section

Starting Materials. Diethylenetriamine (dien), *N*,*N*′,*N*′′-trimethyldiethylenetriamine (*N*,*N*′,*N*′′-Me$_3$dien), *N*,*N*,*N*′,*N*′′,*N*′′-pentamethyldiethylenetriamine (*N*,*N*,*N*′,*N*′′,*N*′′-Me$_5$dien), and Re$_2$(CO)$_{10}$ from Aldrich, *N*,*N*-dimethyldiethylenetriamine (*N*,*N*-Me$_2$dien) from Ames Laboratories, and *N*-methyl-2,2′-diaminodiethylamine (*N*′-Medien) and 2,2′-diaminodiethyl sulfide (daes) from TCI America

(12) Alves, S.; Paulo, A.; Correia, J. D. G.; Gano, L.; Smith, C. J.; Hoffman, T. J.; Santos, I. *Bioconjugate Chem.* **2005**, *16*, 438−449.
(13) Alves, S.; Paulo, A.; Correia, J. D. G.; Domingos, A.; Santos, I. *J. Chem. Soc., Dalton Trans.* **2002**, 4714−4719.
(14) Vitor, R. F.; Alves, S.; Correia, J. D. G.; Paulo, A.; Santos, I. *J. Organomet. Chem.* **2004**, *689*, 4764−4774.
(15) Lipowska, M.; He, H.; Xu, X.; Taylor, A. T.; Marzilli, P. A.; Marzilli, L. G., in preparation.
(16) Lipowska, M.; He, H.; Xu, X.; Marzilli, L. G.; Taylor, A. *J. Labelled Compd. Radiopharm.* **2005**, *48*, S258.
(17) Banerjee, S. R.; Levadala, M. K.; Lazarova, N.; Wei, L.; Valliant, J. F.; Stephenson, K. A.; Babich, J. W.; Maresca, K. P.; Zubieta, J. *Inorg. Chem.* **2002**, *41*, 6417−6425.
(18) Christoforou, A. M.; Marzilli, P. A.; Fronczek, F. R.; Marzilli, L. G. *J. Chem. Crystallogr.*, in press.
(19) Rodríguez, V.; Gutiérrez-Zorrilla, J. M.; Vitoria, P.; Luque, A.; Román, P.; Martínez-Ripoll, M. *Inorg. Chim. Acta* **1999**, *290*, 57−63.
(20) Orpen, A. G. *Chem. Soc. Rev.* **1993**, *22*, 191−197.
(21) Harris, S. E.; Pascual, I.; Orpen, A. G. *J. Chem. Soc., Dalton Trans.* **2001**, 2996−3009.
(22) Schmidtke, H. H.; Garthoff, D. *Inorg. Chim. Acta* **1968**, *2*, 351−356.
(23) Lipowska, M.; He, H. Y.; Malveaux, E.; Xu, X. L.; Marzilli, L. G.; Taylor, A. *J. Nucl. Med.* **2006**, *47*, 1032−1040.

Chart 2

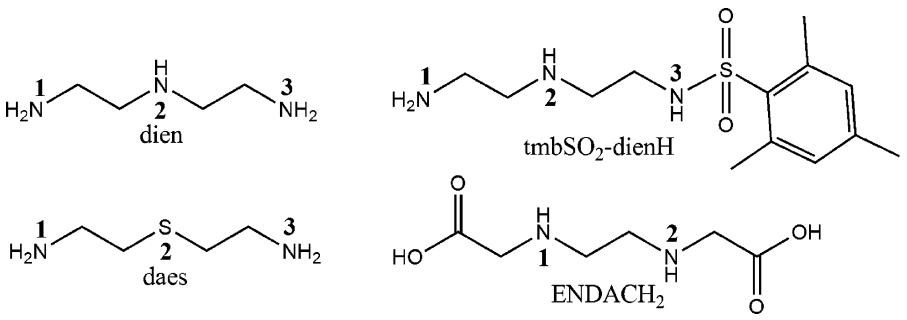

were all used as received. $[Re(CO)_3(H_2O)_3]OTf$ (OTf = trifluoromethanesulfonate)[6] and [Pt(dien)Cl]Cl[24] were prepared by known methods.

NMR Spectroscopy. ^1H NMR spectra were recorded on either 300 or 400 MHz spectrometers. Peak positions are relative to TMS or solvent residual peak, with TMS as the reference. All NMR data were processed with *XWINNMR* and *Mestre-C* software.

X-ray Data Collection and Structure Determination. Single crystals were placed in a cooled nitrogen gas stream at ~100 K on a Nonius Kappa CCD diffractometer fitted with an Oxford Cryostream cooler with graphite-monochromated Mo Kα (0.71073 Å) radiation. Data reduction included absorption corrections by the multiscan method, with *HKL SCALEPACK*.[25] All X-ray structures were determined by direct methods and difference Fourier techniques and refined by full-matrix least-squares, using *SHELXL97*.[26] All non-hydrogen atoms were refined anisotropically. All hydrogen atoms were visible in difference maps but were placed in idealized positions. A torsional parameter was refined for each methyl group.

***fac*-$[Re(CO)_3L]PF_6$ and *fac*-$[Re(CO)_3L]BF_4$.** An aqueous solution of $[Re(CO)_3(H_2O)_3]OTf$ (10 mL, 0.1 mmol) was treated with **L** (0.1 mmol). The pH was adjusted to ~6, and the reaction mixture was heated at reflux for 10 h. The reaction mixture was allowed to cool to room temperature, and the volume was reduced to 5 mL by rotary evaporation. Solid $NaPF_6$ or $NaBF_4$ was added, and the white precipitate that formed was collected on a filter, washed with ether, and dried under vacuum. X-ray-quality crystals were obtained from the filtrate or by slow evaporation from an acetone solution.

$[Re(CO)_3(dien)]PF_6$ (1a). Treatment of the $[Re(CO)_3(H_2O)_3]^+$ (0.1 mmol) solution with dien (10 μL) as described above afforded $[Re(CO)_3(dien)]PF_6$ as a white powder (10 mg, 27% yield) after the addition of $NaPF_6$ (10 mg). The product was characterized by single-crystal X-ray crystallography. ^1H NMR spectrum (ppm) in DMSO-d_6: 6.98 (b, 1H, NH), 5.43 (b, 2H, NH), 4.13 (b, 2H, NH), 2.83 (m, 4H, CH_2), 2.70 (m, 4H, CH_2).

$[Re(CO)_3(dien)]BF_4$ (1b). Treatment of the $[Re(CO)_3(H_2O)_3]^+$ (0.1 mmol) solution with dien (10 μL) as described above afforded $[Re(CO)_3(dien)]BF_4$ as a white powder (9 mg, 19% yield) after the addition of $NaBF_4$ (10 mg). The product was characterized by single-crystal X-ray crystallography. ^1H NMR spectrum (ppm) in DMSO-d_6: identical to that of **1a**.

$[Re(CO)_3(N'\text{-Medien})]_4(PF_6)_3(SO_3CF_3)$ (2). Treatment of the $[Re(CO)_3(H_2O)_3]^+$ (0.1 mmol) solution with *N*′-Medien (12 μL) as described above afforded $[Re(CO)_3(N'\text{-Medien})]PF_6$ as a white powder (17 mg, 44% yield) after the addition of $NaPF_6$ (10 mg). The product was characterized by single-crystal X-ray crystallography. ^1H NMR (ppm) spectrum in DMSO-d_6: 5.59 (b, 2H, NH), 4.17 (b, 2H, NH), 3.13 (s, 3H, Me), 3.08 (m, 2H, CH_2), 2.92−2.66 (m, 6H, CH_2).

$[Re(CO)_3(N,N\text{-Me}_2\text{dien})]PF_6$ (3). Treatment of the $[Re(CO)_3(H_2O)_3]^+$ (0.1 mmol) solution with *N*,*N*-Me_2dien (13 μL) as described above afforded $[Re(CO)_3(N,N\text{-Me}_2\text{dien})]PF_6$ as a white powder (15 mg, 38% yield) after the addition of $NaPF_6$ (10 mg). The product was characterized by single-crystal X-ray crystallography. ^1H NMR (ppm) spectrum in DMSO-d_6: 7.02 (b, 1H, NH), 5.68 (b, 1H, NH), 4.28 (b, 1H, NH), 3.06 (s, 3H, Me), 2.95 (m, 4H, CH_2), 2.76 (s, 3H, Me), 2.75 (m, 4H, CH_2).

***meso-exo*-$[Re(CO)_3(N,N',N''\text{-Me}_3\text{dien})]PF_6$ (*meso-exo*-4).** Treatment of the $[Re(CO)_3(H_2O)_3]^+$ (0.1 mmol) solution with *N*,*N*′,*N*″-Me_3dien (15 μL) as described above afforded the meso-exo isomer of $[Re(CO)_3(N,N'N''\text{-Me}_3\text{dien})]PF_6$ as colorless crystals (9 mg, 22% yield) after the addition of $NaPF_6$ (10 mg). The product was characterized by single-crystal X-ray crystallography. ^1H NMR (ppm) spectrum in DMSO-d_6: 5.22 (b, 2H, NH), 3.18 (s, 3H, Me), 2.97 (m, 4H, CH_2), 2.95 (d, 6H, Me), 2.77 (m, 2H, CH_2).

Solids with the $[Re(CO)_3(N,N,N',N'',N''\text{-Me}_5\text{dien})]^+$ Cation. Treatment of the $[Re(CO)_3(H_2O)_3]^+$ (0.1 mmol) solution with *N*,*N*,*N*′,*N*″,*N*″-Me_5dien (18 μL) as described above followed by the addition of 10 mg of $NaBF_4$ or $NaPF_6$ afforded, respectively, colorless crystals of $[Re(CO)_3(N,N',N',N'',N''\text{-Me}_5\text{dien})]OTf\cdot[Re(CO)_3(\mu_3\text{-}OH)_4]\cdot 3.35H_2O$ (**5**) (10 mg, 36% yield) or a white powder of $[Re(CO)_3(N,N',N',N'',N''\text{-Me}_5\text{dien})]PF_6$ (**5a**) (15 mg, 23% yield). **5a** was recrystallized from acetone, and both crystal types were characterized by single-crystal X-ray crystallography. ^1H NMR (ppm) spectrum of **5a** in DMSO-d_6: 3.23 (s, 6H, Me), 3.21 (m, 4H, CH_2), 3.19 (s, 3H, Me), 3.06 (m, 2H, CH_2), 2.93 (m, 2H, CH_2), 2.81 (s, 6H, Me).

$[Re(CO)_3(daes)]PF_6$ (6). Treatment of the $[Re(CO)_3(H_2O)_3]^+$ (0.1 mmol) solution with daes (10 μL) as described above afforded $[Re(CO)_3(daes)]PF_6$ as crystals (10 mg, 20% yield) after the addition of $NaPF_6$ (10 mg). The product was characterized by single-crystal X-ray crystallography. ^1H NMR (ppm) spectrum in DMSO-d_6: 5.55 (b, 2H, NH), 4.22 (b, 2H, NH), 2.94 (m, 2H, CH_2), 2.75 (m, 6H, CH_2).

Results and Discussion

X-ray Characterization. All complexes exhibit a distorted octahedral structure, with the three carbonyl ligands occupying one face. The remaining coordination sites are occupied by three amines for complexes **1**−**5** (Figure 1) and two amine nitrogens and a thioether sulfur for **6** (Figure 2). Crystal data and details of the structural refinement for complexes **1**−**6** are summarized in Table 1. The Re−N and Re−S bond lengths and the N−Re−N and S−Re−N angles (see Table

(24) Annibale, G.; Brandolisio, M.; Pitteri, B. *Polyhedron* **1995**, *14*, 451−453.
(25) Otwinowski, Z.; Minor, W. *Macromolecular Crystallography, Part A*; New York Academic Press: New York, 1997; Vol. 276.
(26) Sheldrick, G. M. In *Program for Crystal Structure Solution and Refinement*; University of Gottingen: Gottingen, Germany, 1997.

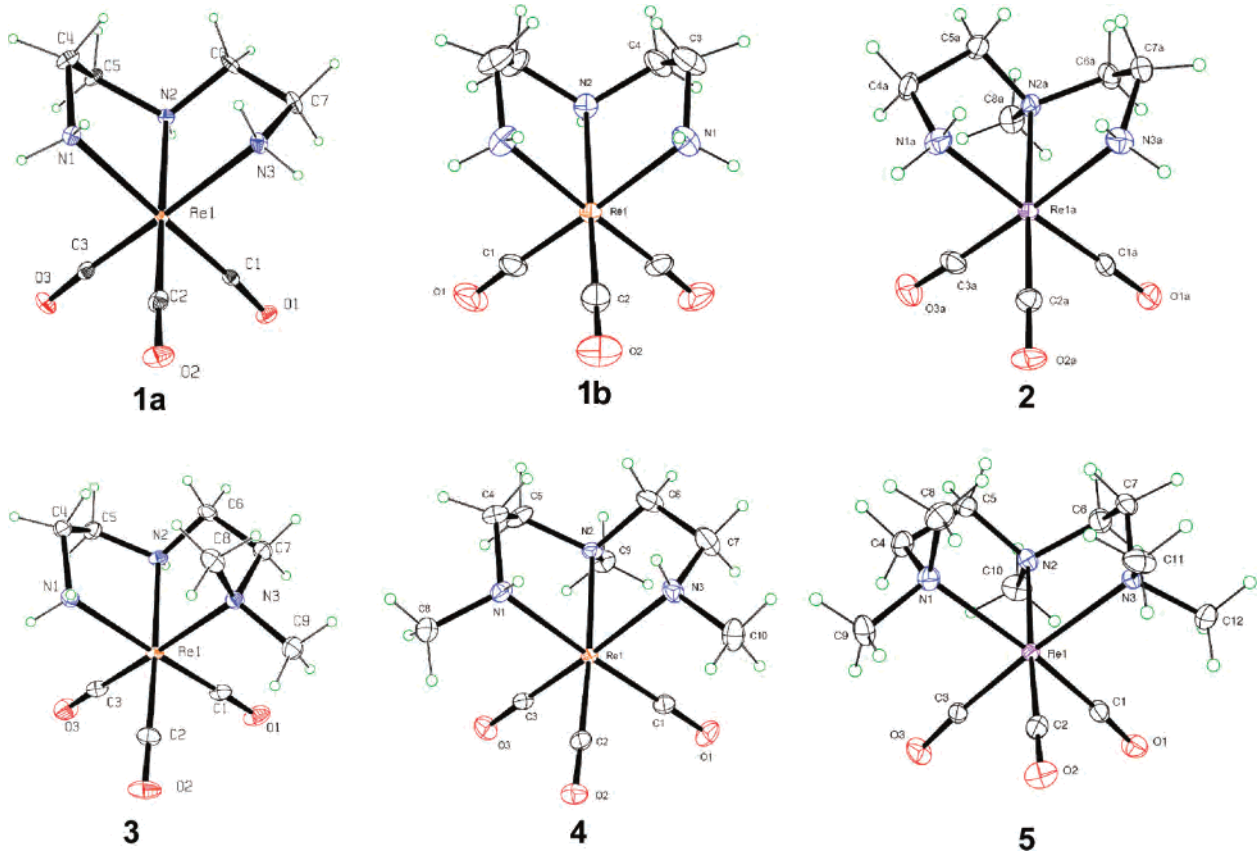

Figure 1. Perspective drawings of **1a**, **1b**, **2**, [**3**, ***meso-exo*-4**, and **5**. Counterions are omitted for clarity. Thermal ellipsoids are drawn with 50% probability.

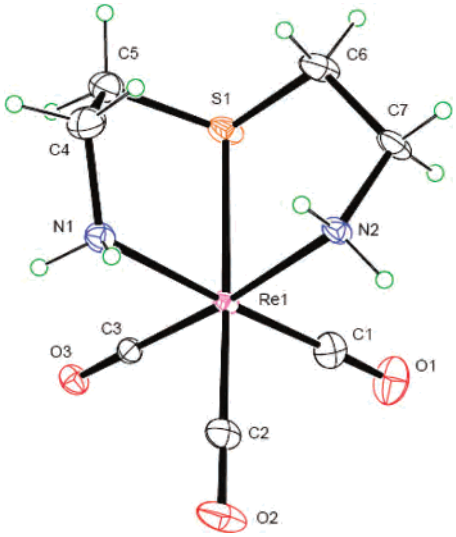

Figure 2. Perspective drawing of **6**. The counterion is omitted for clarity. Thermal ellipsoids are drawn with 50% probability.

2 for selected bond lengths and angles) are comparable to those values of relevant complexes containing amine and thioether groups.[6,7,9,10] Because of the longer Re−S (∼2.2 Å) and C−S (∼1.8 Å) bonds compared with the Re−N (∼2 Å) and C−N (∼1.4 Å) bonds, the S−Re−N chelate ring bite angles and the N−S and C5−C6 nonbonded distances are larger in **6** compared with the respective parameters in **1**−**5** (Table 3). However, near the terminal amines, the structure becomes more similar for the NSN vs the NNN compounds, as illustrated in the Supporting Information. The implication of this result is that pendant groups on terminal amines should project outward in a similar manner for both types of chelates, whereas pendant groups on the carbons adjacent to the donor atom anchoring the two chelate rings will project in a very different manner.

The length of the Re−N bonds depends on the number and size of the substituents replacing the ligand NH groups. The Re−N bonds in complexes in which N1 and N3 have two methyl substituents (**3** and **5**) are significantly longer than any of the other Re−N bonds in **1**−**4**, in which N1, N2, and N3 have at most one methyl substituent replacing an H atom. This lengthening is attributed to the bulkiness of the methyl groups compared with that of the smaller H group. When the amine group has only one methyl group as a substituent, the Re−NHMe bonds are numerically but not significantly longer than the Re−NH_2 bonds. For both the *endo*- and *exo*-[$Re(CO)_3$(ENDACH)] complexes (which crystallize as neutral complexes),[8] the Re−$NHCH_2COOH$ bonds are significantly longer than the Re−NH_2 bond of [$Re(CO)_3$(ENAC)][8] and the Re−NH_2 bonds of the complexes presented here. It is evident that a single methyl group substituent on an amine group probably does not have enough bulk to cause significant lengthening of Re−N bonds, whereas larger substituents (e.g., CH_2COOH in [$Re(CO)_3$-(ENDACH)] in the solid state) or two substituents (e.g., two methyl groups in **3** and **5**) have sufficient bulk to increase the Re−N bonds significantly.

Table 1. Crystal Data and Structure Refinement for **1a**, **1b**, **2**, **3**, ***meso-exo*-4**, **5**, and **6**

	1a	**1b**	**2**	**3**	***meso-exo*-4**	**5**	**6**
formula	$C_7H_{13}N_3O_3$-$RePF_6$	$C_7H_{13}N_3O_3$-$ReBF_4$	4($C_8H_{15}N_3O_3Re$)-$(CF_3O_3S)(PF_6)_3$	$C_9H_{17}N_3O_3$-$RePF_6$	$C_{10}H_{19}N_3O_3$-$RePF_6$	$C_{12}H_{23}N_3ReS$-(CF_3O_3S)-$(C_{12}H_4O_{16}Re_4)$-3.35(H_2O)	$C_7H_{12}N_2O_3$-$ReSPF_6$
fw	518.37	460.21	2133.70	436.43	560.45	588.50	535.42
cryst syst	orthorhombic	monoclinic	monoclinic	orthorhombic	monoclinic	triclinic	orthorhombic
space group	*Pna*2$_1$	*Cm*	*Pc*	*P*2$_1$2$_1$2$_1$	*P*2$_1$/*c*	$P\bar{1}$	*Pna*2$_1$
unit cell dimens							
a (Å)	16.396(2)	9.566(2)	11.4999(6)	8.6289(10)	14.6964(15)	9.6358(10)	12.3209(12)
b (Å)	8.5554(10)	10.267(3)	11.6824(9)	12.0976(13)	13.2755(12)	15.0396(15)	8.3770(10)
c (Å)	9.7512(12)	8.010(2)	22.8706(15)	15.363(2)	17.146(2)	15.4932(15)	14.1136.7(3)
α (deg)	90	90	90	90	90	95.470(5)	90
β (deg)	90	125.730(11)	90.145(4)	90	91.165(4)	98.815(5)	90
γ (deg)	90	90	90	90	90	90.263(5)	90
V (Å^3)	1367.8(3)	638.6(3)	3072.6(3)	1603.7(3)	3344.5(6)	2208.2(4)	1456.7(3)
T (K)	90	173	90	90	90	90	90
Z	4	2	2	4	8	2	4
ρ_{calc} (mg/m^3)	2.517	2.393	2.306	2.263	2.226	2.710	2.441
abs coeff (mm^{-1})	9.084	9.570	8.096	7.754	7.440	13.80	8.670
$2\theta_{max}$ (deg)	72.8	73.6	71.2	80.4	74.0	67.4	73.6
R indices[a]	0.027	0.047	0.036	0.048	0.042	0.036	0.054
wR2 = [$I > 2\sigma(I)$][b]	0.063	0.063	0.083	0.057	0.092	0.087	0.072
data/params	6131/192	2578/99	26464/804	9946/221	15639/452	16677/570	6569/192

[a] $R1 = (\sum||F_o| - |F_c||)/\sum|F_o|$. [b] $wR2 = [\sum[w(F_o^2 - F_c^2)^2]/\sum[w(F_o^2)^2]]^{1/2}$.

Table 2. Selected Bond Distances (Å) and Angles (deg) for **1a**, **1b**, **2**, **3**, ***meso-exo*-4**, **5**, and **6**[a]

	1a	**1b**	**2**	**3**	***meso-exo*-4**	**5**	**6**[a]
				bond distances			
Re−N1	2.238(3)	2.213 (8)	2.197(5)	2.240(2)	2.233(3)	2.233(5)	2.243(5)
Re−N2	2.201(3)	2.222(8)	2.250(4)	2.205(2)	2.238(3)	2.230(4)	2.4737(10)[a]
Re−N3	2.244(3)		2.215(5)	2.265(2)	2.220(3)	2.295(4)	2.226(3)[a]
				bond angles			
N1−Re−N2	77.50(12)	77.9(3)	78.84(18)	77.28(9)	79.62(13)	78.93(16)	80.15(9)[a]
N2−Re−N3	76.56(12)	77.9(3)	77.20(17)	78.65(9)	77.91(13)	79.38(15)	81.06(12)[a]
N1−Re−N3	87.14(12)	87.6(6)	87.8(2)	91.21(9)	86.70(14)	99.15(16)	85.7(2)[a]

[a] For **6**, parameters involving S and N2 are placed in the rows containing N2 and N3 values, respectively.

Table 3. Selected Nonbonded Distances (Å) for **1a**, **1b**, **2**, **3**, ***meso-exo*-4**, **5**, and **6**

complex	pucker	C5H−C6H	C5−C6	C4H−C7H	C4−C7	N1−N2 or N1−S	N2−N3 or N2−S
[Re(CO)$_3$(dien)]Br	*λδ*	2.290	2.514	2.119	3.279	2.790	2.788
1a	*λλ*	2.389	2.478	4.009	3.963	2.754	2.780
1b	*λδ*	2.296	2.524	2.080	3.281	2.787	
2	*δδ*	2.487	2.461	4.272	3.999	2.812	2.797
3	*δδ*	2.485	2.493	4.153	4.029	2.775	2.833
***meso-exo*-4**	*λλ*	2.419	2.458	4.011	3.937	2.840	2.826
5	*δδ*	2.390	2.459	4.128	4.054	2.890	2.902
6	*λλ*	2.616	2.683	3.945	4.010	3.070	3.032

In the solid state of **1b** and **6**, intermolecular hydrogen bonding is observed between the N2H or N1H$_2$ (cf. Figures 1 and 2 for numbering) and a carbonyl group of another molecule in the unit cell (N−O distance = 3.03 Å for **1b** and 2.96 Å for **6**). In complex **2**, hydrogen bonding is observed between the N1H$_2$ group and the OTf counterion (N−O distance = 2.87 Å). No hydrogen bonding was observed in the solid-state structures of **1a** and **3**−**5**. In the [Re(CO)$_3$(dien)]Br crystal, intermolecular hydrogen bonding was observed between one Br$^-$ counteranion and a terminal NH$_2$ group and a central NH of two separate cations.[9]

[Re(CO)$_3$(dien)]X. The [Re(CO)$_3$(dien)]Br salt just mentioned was prepared from $(NEt_4)_2[ReBr_3(CO)_3]$;[9] however, because [Re(CO)$_3$(dien)]$^+$ serves as an important prototypical model complex for elaborated tridentate amine ligands, we synthesized the [Re(CO)$_3$(dien)]$^+$ complex from [Re(CO)$_3$-(H_2O)$_3$]OTf and crystallized both the PF_6^- (**1a**) and the BF_4^- (**1b**) salts. The crystal structure of [Re(CO)$_3$(dien)]Br contains two similar but independent cations in the asymmetric unit. For [Re(CO)$_3$(dien)]Br and [Re(CO)$_3$(dien)]BF_4, the chirality of the pucker differs in the two chelate rings. Overlaying the Re, N1, N2, and N3 atoms of the cation in **1b** with these atoms in the two cations in the Br$^-$ salt gave rms = 0.0101 and 0.0125 Å. For [Re(CO)$_3$(dien)]PF_6, the pucker of both rings has the same chirality. The overlay of the cation in [Re(CO)$_3$(dien)]PF_6 (**1a**) with the two cations in the Br$^-$ salt gave rms = 0.0384 and 0.0378 Å. The difference in the goodness of the fits can be explained because the ring chirality is different in [Re(CO)$_3$(dien)]Br and **1b**, whereas the ring chirality is the same in **1a**.

Solids with the [Re(CO)$_3$(*N*,*N*,*N*′,*N*″,*N*″-Me$_5$dien)]$^+$ Cation. The structure of the [Re(CO)$_3$(*N*,*N*,*N*′,*N*″,*N*″-Me$_5$-

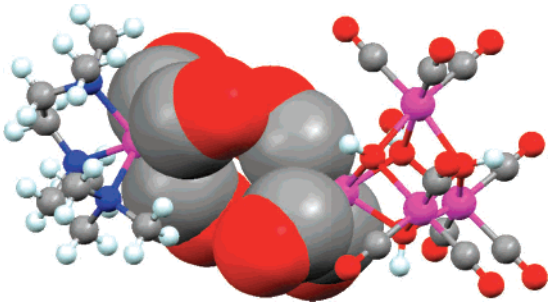

Figure 3. View of the relative orientations of the $[Re(CO)_3(N,N,N',N'',N''\text{-}Me_5dien)]^+$ cation and the neutral $[Re(CO)_3(\mu_3\text{-}OH)]_4$ molecule in the crystal of **5**, showing the interactions of the CO ligands depicted in the space-filling mode.

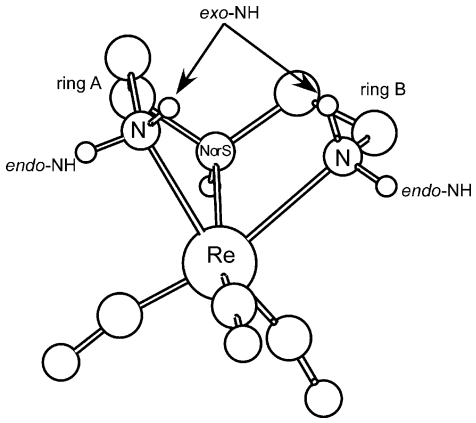

Figure 4. Designation of rings A and B when the structure shown in *ORTEP* is viewed with the nonchelate ring substituent on N2 projecting away from the viewer. Also depicted are the *endo*-NH protons (pointing toward the carbonyl groups) and the *exo*-NH protons (pointing away from the carbonyl groups).

dien)]PF_6 (**5a**) salt was disordered and did not allow analysis of the chirality of the chelate rings. Therefore, we report the crystallographic data only in the Supporting Information. In seeking another salt for obtaining good crystallographic information, we isolated $[Re(CO)_3(N,N,N',N'',N''\text{-}Me_5dien)]$-OTf·$[Re(CO)_3(\mu_3\text{-}OH)]_4$·3.35$H_2O$ (**5**). The $[Re(CO)_3(\mu_3\text{-}OH)]_4$ cubane-type cluster is well known to form in solutions of $[Re(CO)_3(H_2O)_3]^+$ at high pH.[27] In the unit cell, the carbonyl groups of the $[Re(CO)_3(N,N,N',N'',N''\text{-}Me_5dien)]^+$ cation are oriented toward the carbonyl groups of one of the Re atoms of the cluster with O−O nonbonding distances as close as 3.101 Å (Figure 3). The Cambridge Structural Database contains many examples of this cluster but none have a cocrystallized *fac*-$[Re(CO)_3\mathbf{L}]$ complex.

Chirality and Conformation of Chelate Rings. The two rings formed upon dien binding are designated as A (left ring) and B (right ring) in Figure 4. Throughout the text and in Table 3, we report chirality combinations by giving the pucker chirality of ring A, followed by that of ring B for the *ORTEP* structures shown in Figures 1 and 2. The two chelate ring puckers of complexes **2**−**6** have the same chirality, as found for **1a**. Thus, only the **1b** structure has different pucker chirality in each of the two chelate rings, which is the combination most commonly reported. The case of both rings having the same pucker chirality was observed in the $[Re(CO)_3(meso\text{-}LANH)]$ and $[Re(CO)_3(chiral\text{-}LANH)]$ complexes[7] and in the sulfonamido $[Re(CO)_3(DNSH\text{-}dien)]$ complex (DNSH-dienH = *N*-(2-((2-aminoethyl)amino)ethyl)-5-(dimethylamino)naphthalene-1-sulfonamide).[10] The meridionally coordinated ligand in the pseudo-square-planar complex, [Pt(dien)Cl]Cl,[28] has the $\lambda\delta$ chirality combination.

It is obvious from Table 3 that the distance from C4 to C7 is much larger when the pucker chirality is the same in both rings, as it is in complexes **1a** and **2**−**6**, compared with when the ring chirality is different, as it is in **1b** and $[Re(CO)_3(dien)]Br$. The distances between hydrogens or carbons on the two rings when the rings have the same chirality are shorter than the sum of the van der Waals radii for both carbon (3.4 Å) and hydrogen (2.4 Å).[29] This proximity should cause steric repulsion between rings, as suggested by Schmidtke and Garthoff,[22] and their suggestion that the $\delta\delta$ and $\lambda\lambda$ combinations should be favored in fac coordination of the dien ligand seems to be supported by the nonbonded distances. Also, in early molecular mechanics calculations[30] of Co(III) complexes with facially coordinated dien, the $\delta\lambda$ combination was computed to have higher energy than the $\lambda\delta$, $\delta\delta$, and $\lambda\lambda$ combination. pca analyses of X-ray structures of complexes[19,20] find that complexes have different chirality in the two rings more frequently. These analyses were supported by a more recent pca study[21] showing that 74 fragments had the $\delta\lambda$ chirality combination, 16 fragments had the $\lambda\delta$ chirality combination, 18 fragments had the $\delta\delta$ chirality combination, and 18 enantiomeric fragments had the $\lambda\lambda$ chirality combination.

$[Re(CO)_3(N,N',N''\text{-}Me_3dien)]^+$ Isomers. Three $[Re(CO)_3(N,N',N''\text{-}Me_3dien)]^+$ isomers are conceivable (Figure 5). The protons on the terminal amines can be endo (near the carbonyl ligands in the basal plane) or exo (away from the carbonyl ligands), giving the meso-endo isomer (in which both protons point near the carbonyl ligands), the chiral isomer (in which one methyl group points toward and the other away from the carbonyl ligands), and the meso-exo isomer (in which both protons point away from the carbonyl ligands). The synthesis afforded a mixture of the meso-exo (***meso-exo*-4**) and the chiral (***chiral*-4**) isomers, but only the meso-exo isomer was isolated in crystalline form and characterized by X-ray crystallography.

NMR Spectroscopy. The *fac*-$[Re(CO)_3\mathbf{L}]^+$ complexes reported here were characterized by NMR spectroscopy (Table 4) in several solvents (DMSO-d_6, acetone-d_6, and acetonitrile-d_3). For a given solvent, the shifts of the respective terminal NH_2 and central NH signals were similar for all of these complexes. For complexes with terminal primary amino groups (**1**−**3** and the previously reported $[Re(CO)_3(DNSH\text{-}dien)]$[10]), one of the amino group NH signals is unusually upfield. As a result, the amino NH signals of this group have a shift separation (Δ ppm) of 1−1.5 ppm in

(27) Egli, A.; Hegetschweiler, K.; Alberto, R.; Abram, U.; Schibli, R.; Hedinger, R.; Gramlich, V.; Kissner, R.; Schubiger, A. P. *Organometallics* **1997**, *16*, 1833−1840.

(28) Britten, J. F.; Lock, C. J. L.; Pratt, W. M. C. *Acta Crystallogr., Sect. B* **1982**, *B38*, 2148−2155.
(29) Bondi, A. *J. Phys. Chem.* **1964**, *68*, 441−451.
(30) Hambley, T. W.; Searle, G. H. *Aust. J. Chem.* **1984**, *37*, 249−256.

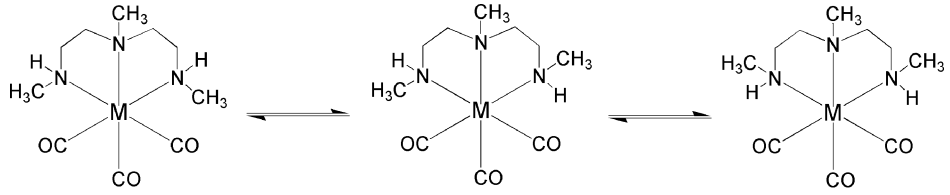

Figure 5. Possible isomers for [Re(CO)$_3$(*N*,*N*′,*N*″-Me$_3$dien)]$^+$.

Table 4. Selected Chemical Shifts (ppm) for **1**, **2**, **3**, ***meso-exo*-4**, ***chiral*-4**, **5a**, and **6** in Various Solvents

	fac-[Re(CO)$_3$**L**]$^+$ complex						
	dien	*N*′-Medien	*N*,*N*-Me$_2$dien	*N*,*N*′,*N*″-Me$_3$dien *chiral*	*N*,*N*′,*N*″-Me$_3$dien *meso-exo*	*N*,*N*,*N*′,*N*″,*N*″-Me$_5$dien	daes
				DMSO-d_6			
exo-N1H/Me	4.14	4.17	4.28/2.76	5.15/2.66	5.15	2.82	4.22
endo-N1H/Me	5.43	5.59	5.68/3.06	6.39/2.94	2.94	3.23	5.54
N2H/Me	6.98	3.13	7.02	3.15	3.18	3.19	
				acetone-d_6			
exo-N1H/Me	4.40	4.37	4.27/3.01	4.74/2.99	5.02	3.08	4.41
endo-N1H/Me	5.22	5.42	5.54/3.30	6.03/3.21	3.21	3.44	5.43
N2H/Me	6.57	3.39	6.64	3.40	3.44	3.43	
				acetonitrile-d_3			
exo-N1H/Me	3.35	3.39	3.25/2.73	3.85/2.72	4.06	2.84	3.39
endo-N1H/Me	4.32	4.43	4.58/3.13	5.04/3.02	3.03	3.27	4.37
N2H/Me	5.57	3.22	5.53	3.21	3.24	3.24	

DMSO-d_6. The [Re(CO)$_3$(*chiral*-LANH)] complex has two NH_2 groups; one group has NH signals with normal chemical shifts of 5.44 and 5.10 ppm (Δ ppm = 0.34) (similar to those of the [Re(CO)$_3$(*meso*-LANH)] complexes), whereas the other NH_2 group has one unusually upfield (3.92 ppm) and one downfield (6.19 ppm) NH signal (Δ ppm = 2.2). Because of the presence of carboxyl groups near the amino groups, interpreting the shifts of the [Re(CO)$_3$(*meso*-LANH)] complexes will require additional fundamental studies beyond the current one. In general, terminal amino groups in Pt and Pd complexes have two signals with Δ ppm values ranging from 0.1 to 0.4.[31,32] Thus, in DMSO-d_6, the relatively downfield NH signal of the amino groups of **1**−**3** all fall in a normal shift range between 5.43 and 5.68 ppm, which is comparable to the shifts (5.11−5.66 ppm) of the respective NH signals of the NH_2 groups in [Pt(DNSH-dien)Cl] and [Pt(dien)Cl]Cl.[31] The upfield shift effect appears to be generally limited to a particular type of NH group in *fac*-[Re(CO)$_3$**L**] complexes.

meso-exo*-[Re(CO)$_3$(*N*,*N*′,*N*″-Me$_3$dien)]PF$_6$ (*meso-exo*-4).** The isomerically pure ***meso-exo*-4** salt in DMSO-d_6 has one set of ^{1}H NMR signals that include one relatively upfield NH signal (integrating to 2 H) at 5.15 ppm (typical chemical shift for secondary amine NH = ∼7 ppm) and one methyl doublet (2.94 ppm). The spectrum remained unchanged even after 2 days. As mentioned above, a mixture of the meso-exo and the chiral isomer of [Re(CO)$_3$(*N*,*N*′,*N*″-Me$_3$dien)]-PF$_6$ (ratio 1:1) was also isolated in the synthesis. The ^{1}H NMR spectrum (DMSO-d_6) of this mixture reveals a relatively downfield (6.39 ppm) small NH signal and a relatively upfield (5.15 ppm) large NH signal, which are respectively assigned to the *endo*-NH of *chiral*-[Re(CO)$_3$-(*N*,*N*′,*N*″-Me$_3$dien)]PF$_6$ (chiral*-4**) and to overlapping signals of the *exo*-NH of ***chiral*-4** and the two *exo*-NH's of ***meso-exo*-4**.

Sodium hydroxide was added to a DMSO-d_6 solution (5 mM, 600 μL) of the pure *meso-exo*-[Re(CO)$_3$(*N*,*N*′,*N*″-Me$_3$-dien)]PF$_6$ crystals in order to base-catalyze isomerization at N1 or N3 of the meso-exo isomer (***meso-exo*-4**) for conversion to other isomers. Upon the addition of base (DMSO-d_6/0.04 M NaOH, 600 μL/10 μL, final [OH$^-$] = 0.6 mM), the NH signal of ***meso-exo*-4** shifted slightly downfield from 5.15 to 5.26 ppm. Thus, the aqueous base caused a slight shift. Within minutes, new signals appeared; these continued to increase for ∼2 h. The new product is clearly ***chiral*-4** with signals having shifts unaffected by aqueous base (see below). The final ratio of the signals of ***chiral*-4** to ***meso-exo*-4** showed that the ***chiral*-4** to ***meso-exo*-4** isomer ratio was 1:1 (the sample was then monitored for 5 months and no further change was observed). A ^{1}H−^{1}H COSY NMR experiment (Supporting Information), allowed the assignment of the signals of the [Re(CO)$_3$(*N*,*N*′,*N*″-Me$_3$dien)]$^+$ isomers. The relatively downfield NH signal of ***chiral*-4** gave a cross-peak to the relatively upfield methyl signal, while the relatively upfield NH signal gave a cross-peak to the relatively downfield methyl signal. By analogy to these assignments, we can assign the unusually upfield NH signal in the spectra of complexes **1**−**3** to the *exo*-NH and the relatively downfield NH signal to the *endo*-NH.

Isomerization of a secondary amine group bound to a Re(CO)$_3$ moiety at high pH was also observed for [Re(CO)$_3$-(ENDAC)]$^-$.[8] The terminal amine substituents are a proton and a dangling acetyl group ($CH_2CO_2^-$). Both isomers were isolated as the neutral [Re(CO)$_3$(ENDACH)] complex. The

(31) Christoforou, A. M.; Marzilli, P. A.; Marzilli, L. G. *Inorg. Chem.* **2006**, *45*, 6771−6781.
(32) Alul, R.; Cleaver, M. B.; Taylor, J.-S. *Inorg. Chem.* **1992**, *31*, 3636−3646.

NH signal of the endo isomer had a chemical shift of 5.84 ppm, whereas the exo isomer had an NH signal at 5.34 ppm in DMSO-d_6. Even though the difference in shift of the two signals is not so large as the difference in shift of the signals of ***chiral*-4** (possibly because of the carboxyl group), the pattern found (relatively upfield *exo*-NH and relatively downfield *endo*-NH signals) is consistent with the pattern found for simpler compounds.

As described above, upon the addition of aqueous base to a DMSO-d_6 sample of pure ***meso-exo*-4**, the *exo*-NH signal shifted downfield (~0.1 ppm, final [OH^-] = 0.6 mM). When only H_2O was added to such a DMSO-d_6 sample, the ***meso-exo*-4** *exo*-NH signal did not shift. The effect of base was also studied with a DMSO-d_6 solution of the isolated noncrystalline mixture of [$Re(CO)_3$(*N*,*N*′,*N*″-Me_3dien)]PF_6. Upon the addition of the same volume of stronger aqueous base (final [OH^-] = 1.7 mM), again only the *exo*-NH signal of ***meso-exo*-4** shifted downfield, and as expected, by a larger amount (~0.5 ppm), whereas the NH signals of ***chiral*-4** remained unchanged. In an essentially identical aqueous base addition experiment with [$Re(CO)_3$(dien)]PF_6, no NH signal shift change was observed.

The downfield shift observed for the *exo*-NH signal of the meso-exo isomer of [$Re(CO)_3$(*N*,*N*′,*N*″-Me_3dien)]PF_6 upon the addition of NaOH might be related to the fact that the two *exo*-NH groups of ***meso-exo*-4** project in the same direction and are relatively fixed in position by the *endo*-Me groups. The ***chiral*-4** isomer has one endo and one exo NH, and the NH groups of [$Re(CO)_3$(dien)]PF_6 may not be at a fixed position because chelate rings are conformationally dynamic. These considerations lead us to suggest that the relatively selective shift effect for ***meso-exo*-4** could be the result of a hydroxo/water solvation cluster bridging the two NH groups. In addition, the absence of such a cluster for the dien complex could be caused by the difference in solvation of the primary amines vs the secondary amines in ***meso-exo*-4**.

Interaction of NH Protons with Cl^- Anion. Understanding the basis of the very different NH shifts of the *fac*-[$Re(CO)_3$**L**] complexes is a challenge. The shift difference we observe could arise from different exposure of the NH group to solvent. To test this possibility, we treated DMSO-d_6 solutions of representative complexes with added Cl^-, an anion known to form H bonds in nonaqueous solvents. If any H bonding occurs between NH and Cl^-, we would expect the NH signal to shift downfield.[33,34]

Indeed, when Cl^- (1 to ~175 mM) was added to a solution of [$Re(CO)_3$(dien)]$^+$ (5 mM, DMSO-d_6), the upfield NH signal assigned to the *exo*-NH groups shifted downfield ($\Delta\delta$ ~ 1.2 ppm) and reached a plateau at ~100 mM of Cl^-, whereas the downfield NH signals assigned to the *endo*-NH's and the central N2H remained relatively unchanged. Figure 6 shows the change in chemical shift ($\Delta\delta$) vs the amount of Cl^- added. Even after the addition of more Cl^-, the *endo*-NH and the central N2H signals do not change significantly. In a similar experiment with [$Re(CO)_3$(daes)]PF_6 (**6**) (2.6 mM, DMSO-d_6), upon Cl^- addition the final $\Delta\delta$ observed was 0.9 ppm (at 100 mM) for the *exo*-NH signal, giving a final shift of 5.13 ppm for the [$Re(CO)_3$(daes)]$^+$,Cl^- ion pair, a value relatively close to the 5.33 ppm observed for the *exo*-NH signal [$Re(CO)_3$(dien)]$^+$,Cl^- ion pair.

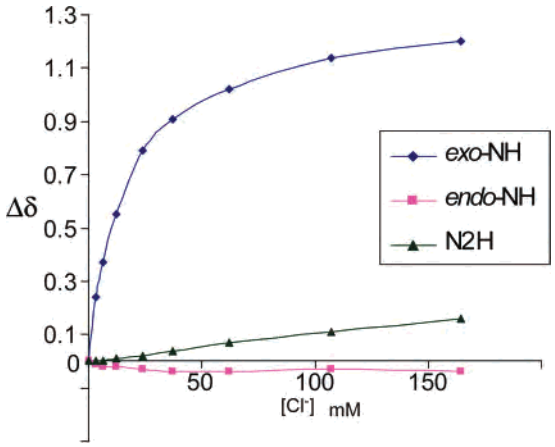

Figure 6. Change in chemical shift ($\Delta\delta$ ppm) of *exo*-NH, *endo*-NH, and N2H signals of [$Re(CO)_3$(dien)]PF_6 upon the addition of Cl^- in DMSO-d_6.

Behavior similar to that of [$Re(CO)_3$(dien)]PF_6 was observed when Cl^- (1 to ~175 mM) was added to a solution of an isomeric mixture of ***meso-exo*-4** and ***chiral*-4** (5 mM, DMSO-d_6). The *exo*-NH signal of ***meso-exo*-4** shifted downfield ($\Delta\delta$ between the final and initial chemical shifts ~1.5 ppm), and the relatively upfield *exo*-NH signal of ***chiral*-4** shifted downfield ($\Delta\delta$ ~ 1.1 ppm). However, the relatively downfield *endo*-NH signal of ***chiral*-4** shifted downfield minimally ($\Delta\delta$ ~ 0.25 ppm). Small changes were also observed in the CH signal of the ethylene chains.

From the data used to plot Figure 6 and the figures in the Supporting Information and assuming that the final ion pair has a 1:1 ratio, we calculated equilibrium constants of 93 ± 5 M^{-1} for [$Re(CO)_3$(dien)]$^+$,Cl^-; 96 ± 11 M^{-1} for [$Re(CO)_3$(daes)]$^+$,Cl^-; and 56 ± 8 and 239 ± 23 M^{-1} for *chiral*- and *meso-exo*-[$Re(CO)_3$(*N*,*N*′,*N*″-Me_3dien)]$^+$,Cl^- ion pairs, respectively. The significantly higher binding constant for ***meso-exo*-4** compared with those of **1** and *chiral*-[$Re(CO)_3$(*N*,*N*′,*N*″-Me_3dien)]$^+$ might be attributed to the fixed location and similar direction of projection of the *exo*-NH's of ***meso-exo*-4**, as discussed above.

In contrast to the above results, when Cl^- was added to solutions of complexes that have only one terminal NH_2 group, the *exo*-NH did not appear to interact strongly with Cl^-. Specifically, when as much as 80 mM Cl^- was added to 5 mM DMSO-d_6 solutions of [$Re(CO)_3$(*N*,*N*-Me_2dien)]-PF_6 and $Re(CO)_3$(DNS-dien),[10] no significant NH shift change was observed. Obviously, at least one NH group in each terminal amine group is necessary in order for selective, localized H bonding with Cl^- to occur.

The downfield shifts by at least 1 ppm of the *exo*-NH signals of **1**, ***meso-exo*-4**, and ***chiral*-4**, attributable to NH···Cl^- hydrogen bonding within the ion pair, correlate roughly with the magnitude of the equilibrium constant.

(33) Marzilli, L. G.; Chang, C.-H.; Caradonna, J. P.; Kistenmacher, T. J. *Adv. Mol. Relax. Interact. Processes* **1979**, *15*, 85−101.
(34) Chang, C.-H.; Marzilli, L. G. *J. Am. Chem. Soc.* **1974**, *96*, 3656−3657.

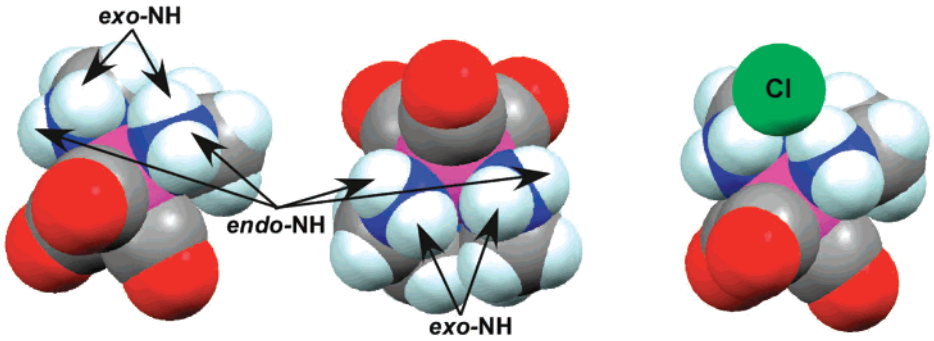

Figure 7. Space-filling model of **1a** showing the orientation of the *exo*-NH and *endo*-NH protons relative to the pocket formed by the ethylene chains of dien. Also shown (right) is the proposed positioning of the Cl$^-$ ion for H bonding between the *exo*-NH protons.

These findings indicate that the Cl$^-$ ion indeed interacts with the two *exo*-NH's in complexes **1**, ***meso-exo*-4**, and **6** and are consistent with the ion pair model for H bonding between Cl$^-$ with the *exo*-NH's proposed in Figure 7. The distances of the Cl$^-$ ion to N1 and N2 (~3.3 Å) are very similar to the distances observed in the solid state for *fac*-[Pt(IV)(dien)-Cl$_3$]Cl,[35] where the Cl$^-$ counterion was H bonded to the two terminal NH$_2$ groups with Cl$^-$ to N distances of 3.252 and 3.245 Å. Consistent with our interpretation of the selective interactions, only small changes in shift of the *endo*-NH, N2H, and CH signals of **1**, ***meso-exo*-4**, and ***chiral*-4** were observed, and these are attributable to nonspecific salt or ionic strength effects.

The effects of Cl$^-$ addition were also examined for acetonitrile-d_3 solutions of [Re(CO)$_3$(dien)]PF$_6$ and of a mixture of *meso-exo*- and *chiral*-[Re(CO)$_3$(*N*,*N*′,*N*″-Me$_3$-dien)]PF$_6$. However, a much lower concentration of Cl$^-$ (20 mM) was necessary to reach the final observed downfield shifts. In this solvent, $\Delta\delta$ had a nearly linear dependence on Cl$^-$ concentration (Supporting Information); therefore, binding constants are too large to be calculated with NMR data. The $\Delta\delta$ values for the *exo*-NH signals of **1**, ***meso-exo*-4**, and ***chiral*-4** (~2.7, 2.4, and 2.7 ppm, respectively) in acetonitrile-d_3 were greater than those in DMSO-d_6 and also greater than for the central N2H signal of [Re(CO)$_3$(dien)]$^+$ and the *endo*-NH signal of ***chiral*-4** ($\Delta\delta \sim 1.3$ and 1.4 ppm, respectively, in acetonitrile-d_3). The final "absolute" chemical shift values of these signals were similar in both DMSO-d_6 and acetonitrile-d_3. This latter finding, combined with the observed larger $\Delta\delta$ values and apparently much larger binding constants for acetonitrile-d_3, can be explained by the weaker hydrogen bonding of this solvent. This property of acetonitrile-d_3 both allows better competition for the NH by Cl$^-$ and leads to a more upfield initial chemical shift position for the NH signals (in turn making $\Delta\delta$ larger). Evidence for this conclusion is found in the Me shifts (Table 4), where the difference in shifts for different solvents is much smaller than that for NH signals, which as noted have shifts reflecting the H-bonding ability of the solvents.

To understand these interactions within the ion pairs better, we examined dien complexes with the ligand coordinated in a meridional fashion. The ^{1}H NMR spectrum of [Pt(dien)-Cl]Cl (DMSO-d_6, 5 mM) exhibits two sets of three NH signals each: an upfield set for [Pt(dien)Cl]$^+$ and a downfield set for [Pt(dien)(Me$_2$SO-d_6)]$^{2+}$.[31] Upon Cl$^-$ (~100 mM) addition to such a solution, the [Pt(dien)(Me$_2$SO)]$^{2+}$ NH signals shifted downfield (from 6.43 and 6.52 ppm to 6.78 and 6.86 ppm, respectively, for the terminal NH$_2$ groups and from 7.10 to 8.66 ppm ($\Delta\delta \sim 1.6$ ppm) for the central NH group). In contrast, for [Pt(dien)Cl]$^+$, the two terminal NH$_2$ signals (5.43 and 5.51 ppm) did not change, and only the central NH signal shifted (from 7.10 to 7.78 ppm, $\Delta\delta \sim 0.7$ ppm). The X-ray structure of [Pt(dien)Cl]Cl (meridional coordination of dien) (unpublished data), suggests that the central NH is somewhat shielded from the solvent by the two ethylene chains (cf. Figure S6 in Supporting Information). Consequently, the central NH group is not readily available to form H bonds with DMSO-d_6. Upon Cl$^-$ addition, we believe that the obstructed central NH group forms H bonds with the relatively small Cl$^-$ ion (vs the bulkier DMSO-d_6). In contrast, analysis of the X-ray structure of *fac*-[Re(CO)$_3$(dien)]$^+$ suggests that the central NH group will be relatively exposed to the solvent (the two ethylene chains project away from the central NH, cf. Figure S6 in Supporting Information). Thus, the central NH group is available for H bonding with the solvent, disfavoring interaction with the Cl$^-$ ion. The insignificant change in chemical shift of the terminal NH$_2$ signals in [Pt(dien)Cl]$^+$ is attributed to the presence of the chloro ligand creating a localized negatively charged region that inhibits Cl$^-$ ion interaction near the terminal NH$_2$ groups. Also, in [Pt(dien)-(Me$_2$SO)]$^{2+}$ the bulky Me$_2$SO ligand prevents strong interaction of the Cl$^-$ ion with the terminal NH$_2$ groups. Thus, contrary to what is observed for the *fac*-[Re(CO)$_3$**L**]$^+$ complexes, the interaction of the Cl$^-$ ion at the central NH group of Pt(dien) complexes is more favorable than at the terminal amines.

The locations of the NH protons of the terminal amines of various *fac*-[Re(CO)$_3$**L**] structures indicate to us that in solution the *exo*-NH's are somewhat protected from the solvent, whereas the *endo*-NH's are more exposed to the solvent. Space-filling models of the X-ray structures show that the *exo*-NH proton points slightly toward the pocket formed by the ethylene chains of **L** (Figure 7). In contrast, the *endo*-NH proton, which points toward the carbonyl ligands and away from any **L** bulk, appears to be more

(35) Britten, J. F.; Lock, C. J. L. *Acta Crystallogr., Sect. B* **1980**, *B36*, 2958−2963.

exposed to the solvent. The X-ray structure of [Pt(dien)Cl]-Cl (unpublished data) indicates that the *exo*- and *endo*-NH protons should have a similar exposure to solvent, explaining the much smaller difference in the chemical shift of the two NH signals compared with the difference observed for *fac*-[$Re(CO)_3$**L**] complexes.

Conclusions

The simple prototypical ligands studied here bind to the *fac*-$Re(CO)_3$ core in tridentate mode, giving cations of the *fac*-$[Re(CO)_3\mathbf{L}]^+$ type. Most complexes reported here have the same chirality in each chelate ring, a finding in accord with our observation that less severe steric clashes between rings would occur when both rings have the same chirality. However, our results are in surprising contrast to surveys of the literature showing that complexes of the *fac*-M(dien) type with different chirality occur more often. An interesting finding was the downfield shifting of the *exo*-NH's of the *meso-exo*-$[Re(CO)_3(N,N',N''\text{-}Me_3dien)]PF_6$ complex upon the addition of base. This effect might be caused by the formation of a hydroxo/water solvation bridge between the two *exo*-NH's, which probably are in a relatively fixed position in this meso-exo isomer. The addition of Cl^- caused downfield shifting of the relatively upfield *exo*-NH's of $[Re(CO)_3(dien)]^+$, $[Re(CO)_3(daes)]^+$, and two isomers of $[Re(CO)_3(N,N',N''\text{-}Me_3dien)]^+$, suggesting that hydrogen bonding occurs between the *exo*-NH's and the Cl^- ion. This finding indicates that the *exo*-NH groups are protected from the solvent environment and therefore have relatively upfield chemical shifts compared with those of the *endo*-NH groups. Although relatively few other studies of anion interactions with complexes related to those studied here have appeared, a fairly comprehensive set of studies provides results consistent with our finding that these interactions are stronger in acetonitrile.[36−39]

Our work indicates that in designing an NSN ligand, the pendant groups are more likely to be differently positioned than in the NNN analogues if they are placed closer to the thioether. Also, terminal secondary amines have normal Re−N distances for a small substituent such as methyl, but bulkier substituents affect bond length. An unforeseen implication of our work is that the NH group in such secondary amines may be more rigidly positioned, affecting solvation and hence biodistribution. In this regard, it would be informative to evaluate analogues with bulkier substituents[40] by means of the "Cl^- probe" approach described herein.

In summary, the interactions of the various ligand groups in tracer metal complexes influence biodistribution and must be understood to improve methods of targeting such tracers. NMR methods are among the best approaches for assessing interactions of tracer complexes in solution. The types of analysis that we have presented can be viewed as being in their infancy. Some of the unusual and as yet incompletely explained NMR shifts of Re analogues of ^{99m}Tc tracers very probably reflect differences in solvation of the various parts of the bound ligands. We believe that additional NMR/structural investigations similar to the present study will be needed to strengthen the knowledge base needed to design tracers rationally.

Acknowledgment. This investigation was supported by funds from LSU and by NIH Grant DK 38842 (to Andrew Taylor, Emory University, as PI). Purchase of the diffractometer was made possible by Grant No. LEQSF(1999−2000)-ENH-TR-13, administered by the Louisiana Board of Regents.

Supporting Information Available: Plots showing dependence on Cl^- ion concentration of $\Delta\delta$ of NH signals of $[Re(CO)_3(dien)]PF_6$ and ***chiral*-4** and ***meso-exo*-4** in acetonitrile-d_3 and $[Re(CO)_3(daes)]PF_6$, ***chiral*-4**, and ***meso-exo*-4** in DMSO-d_6; overlay illustration of $[Re(CO)_3(daes)]^+$ and $[Re(CO)_3(N'\text{-Medien})]^+$ cations; orientation of the central NH group in [Pt(dien)Cl]Cl and $Re(CO)_3(dien)]PF_6$; ^1H-^1H COSY NMR spectrum of ***meso-exo*-4** and ***chiral*-4** (mixture obtained upon isomerization with base); crystallographic data for **1a**, **1b**, **2**, **3**, ***meso-exo*-4**, **5**, **5a**, and **6** in CIF format. This material is available free of charge via the Internet at http://pubs.acs.org.

IC701576U

(36) Nieto, S.; Perez, J.; Riera, L.; Riera, V.; Miguel, D. *Chem.—Eur. J.* **2006**, *12*, 2244−2251.
(37) Nieto, S.; Perez, J.; Riera, L.; Riera, V.; Miguel, D. *New J. Chem.* **2006**, *30*, 838−841.
(38) Nieto, S.; Perez, J.; Riera, L.; Riera, V.; Miguel, D.; Golen, J. A.; Rheingold, A. L. *Inorg. Chem.* **2007**, *46*, 3407−3418.
(39) Ion, L.; Morales, D.; Nieto, S.; Perez, J.; Riera, L.; Riera, V.; Miguel, D.; Kowenicki, R. A.; McPartlin, M. *Inorg. Chem.* **2007**, *46*, 2846−2853.
(40) Hafliger, P.; Agorastos, N.; Spingler, B.; Georgiev, O.; Viola, G.; Alberto, R. *ChemBioChem* **2005**, *6*, 414−421.